View Article Online / Journal Homepage / Table of Contents for this issue
Dynamic Article Links

Journal of
Materials Chemistry

Cite this: *J. Mater. Chem.*, 2012, **22**, 24637

www.rsc.org/materials

PAPER

Novel efficient catalysts based on imine-linked mesoporous polymers for hydrogenation and cyclopropanation reactions

Ester Verde-Sesto,[a] Eva M. Maya,*[a] Ángel E. Lozano,[a] Jose G. de la Campa,[a] Félix Sánchez[b] and Marta Iglesias*[c]

Received 25th July 2012, Accepted 27th September 2012
DOI: 10.1039/c2jm34927b

Two imine-linked polymer organic frameworks (**POFs**) with different geometries (**C3v-POF** and **Th-POF**) and mesoporous properties were prepared and proved to be catalyst supports. Due to the greater ability of **Th-POF** to coordinate metals, Cu- and Ir-coordinated **Th-POFs** were tested as catalysts. Both act as truly heterogeneous catalysts towards cyclopropanation and hydrogenation of alkenes, respectively. The high surface area and easy accessibility to the catalytic sites make these materials very efficient for heterogeneous catalysis. The stability of the coordinated complexes and the porous frameworks allows several reuses with only a minor loss in catalytic activity.

1. Introduction

During the last decade mesoporous materials have been paid much attention owing to their great potential in practical applications such as catalysis, gas adsorption, sensing and separations.[1] One of the most recent breakthroughs in this field is the synthesis of mesoporous organic polymers. In general, they can be prepared by phase separation[2,3] using a hard template approach,[4,5] and more recently using amphiphilic surfactants and block copolymers or oligomers.[6–9]

The direct polycondensation of tri- or tetrafunctional monomer and difunctional reagents to achieve porous polymers has been less explored, because it habitually leads to polymer gels or highly cross-linked materials which are insoluble, which complicates their processability and therefore limits their applications.[10] To date, most of the studies reporting direct condensation between tri and difunctional monomers have been performed to get hyperbranched polymers for applications such as additives or dispersants.[11–15] However, by using the appropriate monomer structure and tuning of reaction conditions these cross-linked polymers may form porous structures with interesting potential applications, such as gas storage or catalyst support.[16–18] The pore dimensions and the surface areas have been controlled through the monomer structure to achieve microporous polymers. For example, Jiang *et al.* have reported a series of conjugated polymer and copolymer networks with surface areas in the range of 500–1000 $m^2\ g^{-1}$ by direct coupling of $A_3 + B_2$ monomers of different lengths.[19]

In 2009, Uribe-Romo *et al.* reported a new class of crystalline material that was formed by condensation of a tetrahedral monomer, tetra-(4-aminophenyl)methane, and 1,4-benzenedicarbaldehyde. The 3D crystalline framework formed imine-linked polymer organic frameworks (**POFs**) exhibiting microporosity with a surface area of 1360 $m^2\ g^{-1}$ and a pore size of 0.78 nm.[20] Later, Pandey *et al.* reported the condensation between a C_{3v}-symmetrical monomer, 1,3,5-triformylbenzene, and several diamines to yield amorphous microporous imine-**POFs** with high specific surface areas (from 500 to 1500 $m^2\ g^{-1}$), and also described their use for gas storage.[21] One of these polyimines has been recently synthesized by Ding *et al.* who gave a step further and reported the first application of a Pd(II) containing porous polyimine in Suzuki–Miyaura coupling reactions. The palladium was coordinated to two imine bonds yielding a two-dimensional layered sheet structure. They have demonstrated the higher activity of this material by the excellent yields obtained as well as the recyclability of the catalysts.[22]

In the first part of this work we report the synthesis and characterization of two new mesoporous polymers (**POFs**) through interlinking of strong covalent imine bonds, using 1,4-benzenedicarbaldehyde and two amines of different geometries: one with a C_{3v} symmetry and the second one with a tetrahedral geometry (T_h) (Scheme 1).

These covalent imine frameworks offer a large number of metal binding sites for post-functionalization. Thus, in the second part of this study we report on the most important contribution of this paper, namely the incorporation of coordinated copper- or iridium-complexes into these **POFs** and

---

[a] *Departamento de Química Macromolecular Aplicada, Instituto de Ciencia y Tecnología de Polímeros, Consejo Superior de Investigaciones Científicas (CSIC), Juan de la Cierva 3, Madrid 28006, Spain. E-mail: evamaya@ictp.csic.es; Fax: +34 915644853; Tel: +34 915622900 ext. 457*
[b] *Departamento de Síntesis, Estructura y Propiedades de Compuestos Orgánicos, Instituto de Química Orgánica General, CSIC, Juan de la Cierva 3, Madrid 28006, Spain. E-mail: felix-iqo@iqog.csic.es; Fax: +34 915644853; Tel: +34 915622900 ext. 258*
[c] *Departamento de Nuevas Arquitecturas en Química de Materiales, Instituto de Ciencia de Materiales de Madrid, CSIC, Sor Juana Ines de la Cruz 3.Cantoblanco, Madrid 28049, Spain. E-mail: marta.iglesias@icmm.csic.es; Fax: +34 913720623; Tel: +34 913349000 ext. 101*

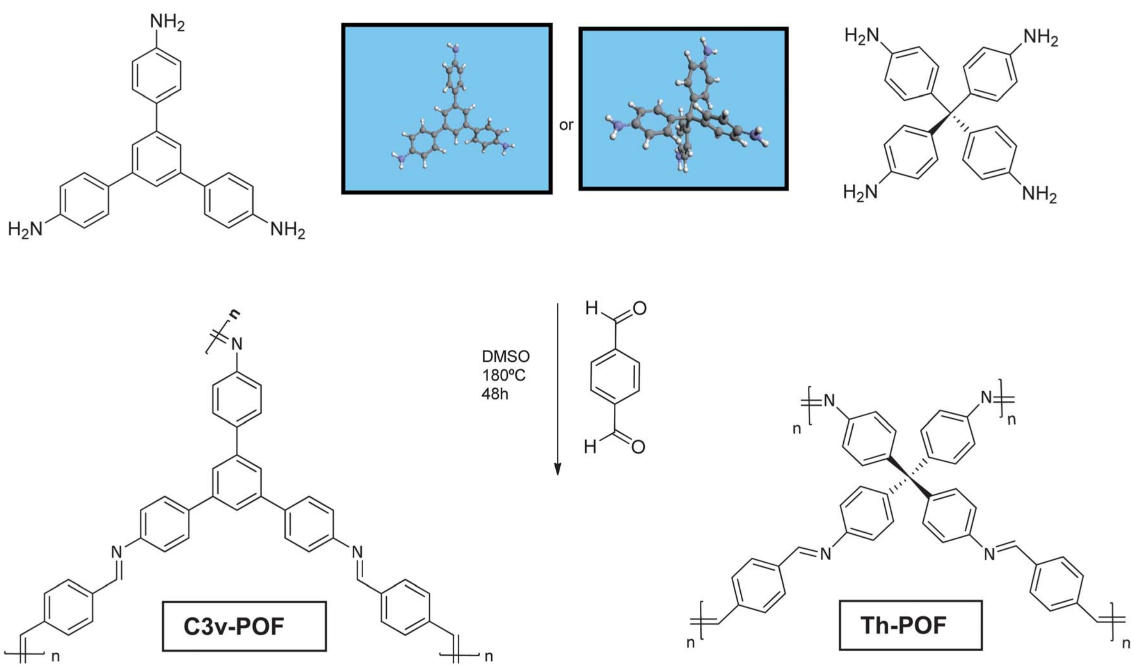

Scheme 1 Synthesis and structure of the imine-linked mesoporous polymer organic frameworks (**POFs**) of this work.

subsequently their catalytic performance in cyclopropanation and hydrogenation reactions.

2. Results and discussion

2.1 Synthesis and characterization of imine-linked POFs

The synthesis of the novel imine-**POFs** was carried out by combining 1,4-benzenedicarbaldehyde with the triamine 1,3,5-tris(4-aminophenyl)benzene (C_{3v}) or with the tetra-(4-aminophenyl)methane (T_h) (Scheme 1).

The IR spectra of both polymers showed the strong C=N band at 1620 cm^{-1} characteristic of the imine groups but also the remaining weak bands at 1690 cm^{-1} and 3400 cm^{-1}, which indicated the presence of small amounts of unreacted aldehyde or amine groups. This result was in agreement with the work reported by Pandey *et al.*, who detected also unreacted groups in a similar condensation.[21]

The corresponding polymers, **C3v-POF** and **Th-POF**, were first characterized by BET. Both polymers exhibited mesoporous properties with similar specific surface areas of 438 and 410 $m^2\ g^{-1}$ respectively: However, the average pore diameters and pore volumes were quite different for both compounds being significantly higher for **Th-POF** (Table 1).

Moreover, the isothermals (Fig. 1) revealed that the accessibility of N_2 to the pores of **C3v-POF** was much more restricted.

Table 1 Pore properties of imine-linked **POFs**

Polymer	Surface areas ($m^2\ g^{-1}$)	Aver. pore size (nm)	Pore vol. ($cm^3\ g^{-1}$)
C3v-POF	438	3	0.07
Th-POF	410	21	1.18
Cu-Th-POF	309	25	1.43
Ir-Th-POF	172	18	0.54

The thermal properties of both compounds were evaluated in air atmosphere using TGA. Both materials exhibited very high thermal stability with decomposition temperatures above 400 °C.

Regarding the morphology, it was observed by WAXS that these **POFs** were amorphous and the SEM showed typical porous morphology with some agglomerates and spherical structures (Fig. 2).

The quantities of nitrogen, determined by elemental analysis, were in agreement with the proposed structures.

2.2 Preparation and characterization of novel catalysts

Through a simple post-treatment of **C3v-POF** or **Th-POF** with CuCl, $CuCl_2$ or $[IrCl(COD)_2]$ (Scheme 2), metal complex-containing **POF** materials (**M-POF**) were easily prepared (see the Experimental part).

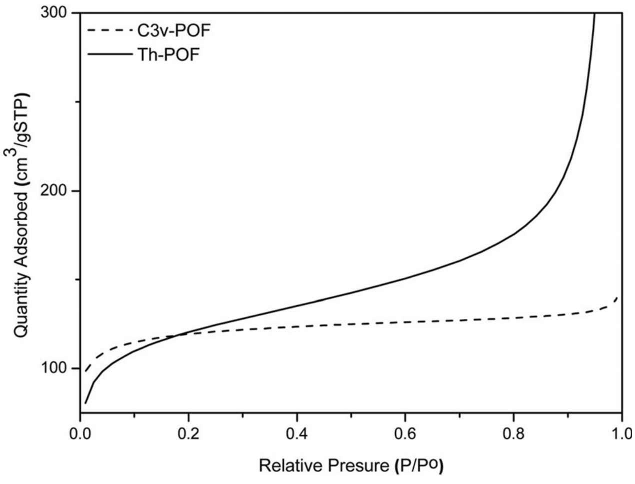

Fig. 1 Nitrogen adsorption isotherm of imine-**POFs**.

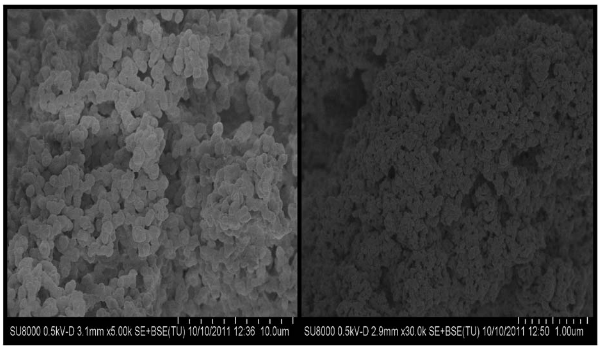

Fig. 2 SEM images of **C3v-POF** (left) and **Th-POF** (right).

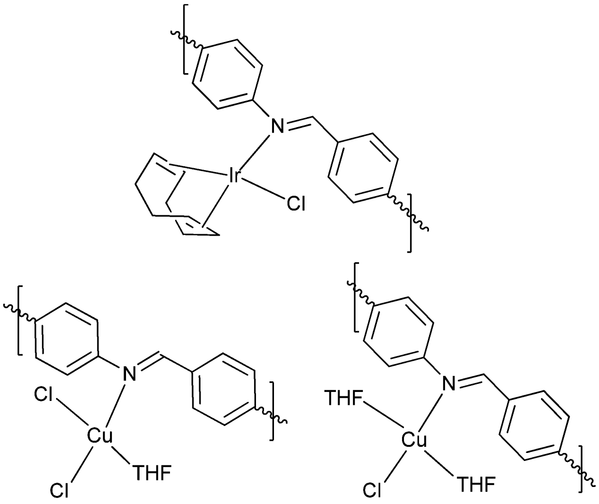

Scheme 2 Post synthetically modificated, **M-Th-POF**: M= ClCODIr(I), Cl(Solv)$_2$Cu(I), Cl$_2$SolvCu(II).

The analysis by ICP of the content of metal incorporated to the imine-**POF** revealed that **C3v-POF** showed lower metal binding ability than **Th-POF**. Thus the amounts of copper(II) and iridium introduced in the C_{3v} material were only 0.41 and 0.39 wt% respectively, whereas the **Th-POF** showed 2.73 wt% of copper(II) and 2.70 wt% of iridium. These results are in agreement with the lower pore volume found by BET for **C3v-POF**.

According to these results, Cu(I) was introduced only in the **Th-POF**. Thus the catalysis experiments were carried out only with metal complexes of this support.

A comparison of the WAXS patterns (Fig. 3) of **Th-POF** and **M-Th-POF** revealed that the structure of **Th-POF** was well preserved after the treatment with [IrCl(COD)$_2$] and CuCl$_2$. However, we have found that the material functionalized with copper(I) presents some peaks of crystallinity. Taking into account that coordination of a metal ion to the C=N nitrogen lone pair suppresses C=N isomerization,[23,24] the peaks of crystallinity observed in this complex could be attributed to the coordination of a copper atom with two imine bonds that might be causing a certain ordering in this structure. The coordination of a metal with two imine bonds was previously observed by Ding *et al.* in porous polyimines, although it was palladium(II) coordinated to a polyimine synthesized from a C_{3v} monomer.[22]

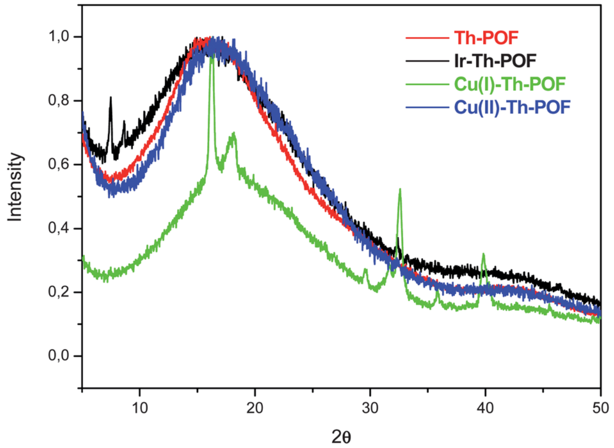

Fig. 3 WAXS patterns of **Th-POFs**.

In order to understand this behaviour, UV-vis spectra of **Th-POFs** were recorded (Fig. 4). In the case of **Th-POF**, two absorption maxima appeared around 280 and 350 nm caused by π–π* and *n*–π* states respectively, as was previously reported for conjugated aromatic imine systems.[25] **Ir-Th-POF** showed similar electronic spectra to those of **Th-POF**, which indicated that iridium did not alter in any extent the electronic density of the C=N bonds. However, electronic spectra of **Cu(I)-** and **Cu(II)-Th-POFs** were quite different from those of the **Th-POF** and iridium complex. Besides the bands due to the imine bonds, **Cu(II)-Th-POF** exhibited a broad shoulder around 600 nm, nonexistent in the **Cu(I)-Th-POF**. This shoulder at 600 nm has been previously observed in conjugated aromatic polyimines bearing electron withdrawing side groups.[26] Thus, copper(I) and copper(II) could be modifying the electronic density of the imine bonds differently.

The pore properties and thermal behavior were evaluated only for the metal supports that were tested in catalysis, **Cu(I)-Th-POF** and **Ir-Th-POF**.

As shown in Table 1, the incorporation of Cu(I) reduced the surface area while a slight increase in the average pore size and pore volume was observed. For the Ir-complex, the surface area was lower than that of the Cu-complex, which could be

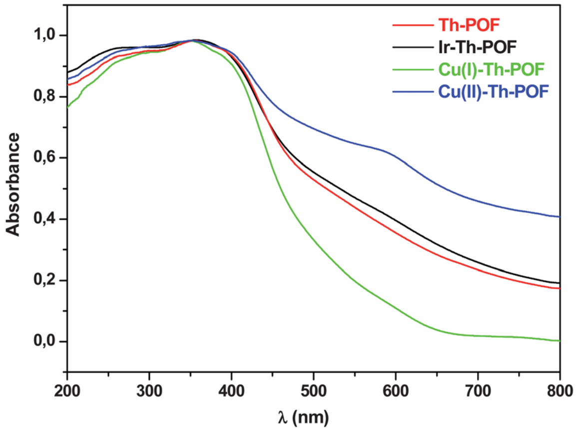

Fig. 4 Optical absorption spectra of **Th-POFs**.

attributed to the different geometries of both metal complexes. In fact, the comparison between the isothermals (Fig. 5) showed that the accessibility of N_2 to the pores of **Th-POF** and the copper complex was similar. However, the nitrogen adsorption of the iridium complex was more difficult.

The thermograms obtained by TGA revealed that metal reduced the thermal stability of the **Th-POF** (Fig. 6) at about 100 °C for the **Ir-Th-POF** and 140 °C in the case of **Cu(I)-Th-POF**. This fact can be attributed to the presence of ligands which reduces the thermal stability as it was reported for polymer complexes with some transition metal chlorides and acetates.[27]

2.3 Catalysis

2.3.1 Cyclopropanation reaction. The catalytic activity of Cu-loaded imine-functionalized material **Cu-Th-POF** was tested for the liquid-phase cyclopropanation reaction over various alkenes (eqn (1)).

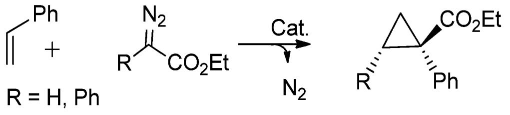

(1)

In the first experiments we compared the catalytic activity of both **Cu(I)** and **Cu(II)-Th-POFs** using styrene and ethyl diazoacetate. The results showed that the material containing Cu(I) was much more active. Thus all cyclopropanation reactions were performed in the presence of Cu(I) (designated as **Cu-Th-POF**).

In the initial stage of our work, we have focused on control experiments to optimize suitable conditions for an efficient and mild catalytic cyclopropanation using ethyl diazoacetate (EDA) in the presence of **Cu-Th-POF**. To perform these initial studies, styrene was chosen as a model substrate. First, a diazo compound was slowly added over 2 h to the reaction mixture containing catalyst and olefin, using a syringe pump. GC and GC-MS analyses of the reaction mixtures showed that *cis–trans* cyclopropane mixtures are formed as the main products of these reactions (50–70%, 100% at higher reaction times, 72 h, Table 3, entry 1), together with minor amounts of coupling products. Second, a **Cu-Th-POF**-catalyzed carbene transfer reaction was carried out in the absence of solvent. In this case, the cyclopropanecarboxylates were obtained with low selectivity due to the formation of relatively large amounts of dimerization products, together with *o*-, *m*-, *p*-aromatic addition products. Third, the diazoacetate was added at once, and it was observed that the reactivity and selectivity of the reaction is similar to that obtained when it is added slowly (entry 2, Table 2). Therefore, the reactions are carried out in dichloromethane at room temperature and the diazo compound is added at once. The activity of the catalyst in this transformation can be estimated on the basis of the time required for the complete consumption of the alkene. Comparison with other previously reported heterogenized Cu-catalysts [supported complexes on USY zeolite and mesoporous MCM-41 matrices (Cu-USY, Cu-MCM-41)][28] shows that **Cu-Th-POF** displays similar rates and selectivity, as can be seen in Table 2.

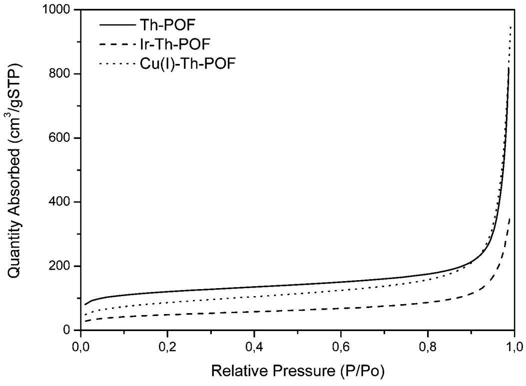

Fig. 5 Nitrogen adsorption isotherm of **Th-POF** compared with their metal complexes.

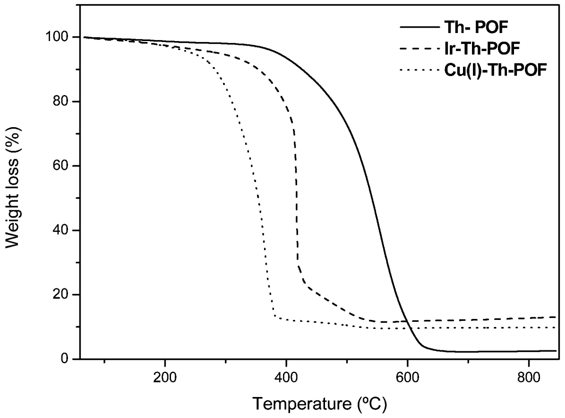

Fig. 6 TGA curves of **Th-POF** and **M-POFs**.

The **Cu-Th-POF**-catalyzed styrene cyclopropanation reaction with ethyl phenyldiazoacetate (PhEDA) provided better results, as shown in Table 3 (entry 2). A unique diastereoisomer (*trans*-Ph/COOEt) was obtained, similarly to other systems reported for this substrate with this diazo compound. The reaction times required for complete diazo consumption are similar to those for EDA.

The optimized protocol was extended to other substrates to determine the scope of the catalytic activity of **Cu-Th-POF** and also to study the chemoselectivity and diastereo selectivity of the cyclopropanation. We tested three types of olefins, styrene, a linear alkene (1-octene) and a cyclic olefin (dihydropyrane), using EDA as cyclopropanating agents (Table 3). Yields were moderate for 1-octene. In contrast, **Cu-Th-POF** exhibited a remarkable diastereoselectivity in the cyclopropanation of the cyclic olefin. In the case of dihydropyrane, a 100 : 0 *trans* : *cis* ratio was achieved.

Reusability experiments conducted with **Cu-Th-POF** demonstrated that the catalyst is stable and no loss of either activity or selectivity was detected for the cyclopropanation of styrene. Table 4 shows that conversions and yields of *cis*- and *trans*-products derived from styrene were maintained within four cycles.

The reusability of the material, together with the fact that the metal loading (as determined by ICP-AES) remained unchanged after the fourth cycle, excludes the occurrence of metal leaching from the solid to the liquid. To confirm the heterogeneity of the

Table 2 Catalytic results for the cyclopropanation reaction involving styrene and ethyl diazoacetates

Entry	Cat.[a]	Diazo compound	%conv. (h)	dr[b] (%)
1	**Cu-Th-POF**	EDA (slowly added, 2 h)	51, (24)	79
2	**Cu-Th-POF**	EDA (added at once)	42, (24)	75
3	**Cu-USY**[27]	EDA (slowly added, 2 h)	32, (20)	55
4	**Cu-MCM-41** (ref. 27)	EDA (slowly added, 2 h)	60, (21)	59

[a] 5–10 mol% catalyst loading. [b] Diastereomeric ratio excess (*trans* − *cis*/*trans* + *cis*).

reaction, in a control experiment the reaction was stopped after 1 h, and after filtration of the solid, the Cu content in the filtrate was analyzed. ICP-AES analysis revealed that metal leaching was negligible. The reaction was tried with the filtrate, but no further conversion was observed. No dissolved active species are thus assumed to be present in reaction mixtures with the **Cu-Th-POF**, and the catalytic activity can be associated to the **POF** structure.

2.3.2 Hydrogenation reactions.

The catalytic activity of the **Ir-Th-POF** compound for the hydrogenation of alkenes was evaluated. Reactions were carried out in ethanol at 40 °C, 2 bar P_{H_2}. Table 5 and Fig. 7 summarize the results wherein the compounds were reduced with excellent yields. A range of alkenes were used as substrates.

To investigate the heterogeneous nature of the catalysis taking place in our system, the heterogenized **Ir-Th-POF** catalyst could be reused several times with a conversion range of 98% (Fig. 8, Table 6). This was also supported by ICP analysis that only a trace amount of iridium (0.02%) was observed in the reaction liquid. Thus, it indicated that slight leaching into the solution occurred.

Table 3 Catalytic results for the cyclopropanation reaction involving alkenes and alkyl diazoacetates[a]

Entry	Alkene	Diazo-compound	%conv. (h)	dr[b] (%)
1	Styrene	EDA	42 (24) 100 (72)	75
2	Styrene	PhEDA	65 (24) 89 (72)	100
3	Dihydropyrane	EDA	50 (24) 80 (72)	100
4	1-Octene	EDA	24 (24) 55 (72)	74

[a] 10 mol% catalyst loading. [b] Diastereomeric ratio excess (*trans* − *cis*/*trans* + *cis*).

Table 4 Recycling results for the cyclopropanation of styrene with ethyl diazoacetate (EDA)

Entry	Conv. (24 h)	*Cis*/*trans*[a]
1	51	38/62
2	67	37/63
3	74	33/67
5	63	36/64

[a] Selectivity towards cyclopropane carboxylates.

Table 5 Catalytic results for the **Ir-Th-POF**-catalyzed hydrogenation reaction[a]

Entry	Alkene	%conv. (h)	TOF[b]
1	Styrene	95 (8.00)	323
2	α-Methyl styrene	86 (8.00)	271
3	1-Octene	100 (0.17)	5880

[a] 0.1 mol% catalyst loading. [b] mmol cat./mmol subs. h

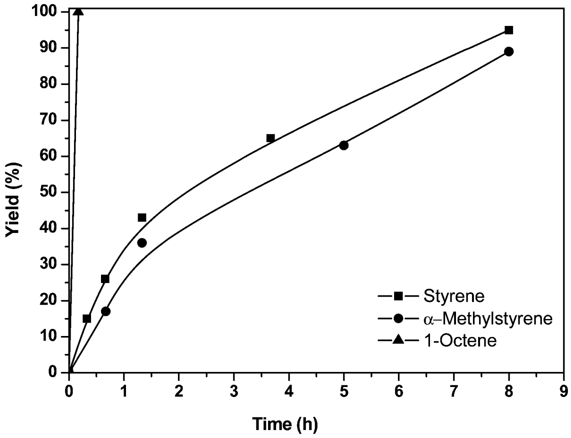

Fig. 7 Kinetic profile for **Ir-Th-POF**-catalyzed hydrogenation of alkenes.

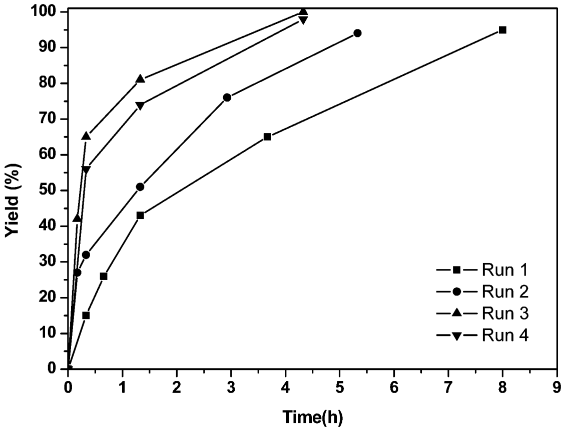

Fig. 8 Kinetic profile for recycling experiments: **Ir-Th-POF**-catalyzed hydrogenation of styrene.

Table 6 Recycling experiments for the **Ir-Th-POF**-catalyzed hydrogenation of styrene

Run	%conv., t (h)	TOF[a]
1	95, (8.00)	323
2	94, (5.33)	1588
3	100, (4.33)	2470
4	98, (4.33)	1697

[a] mmol subs./mmol cat. h.

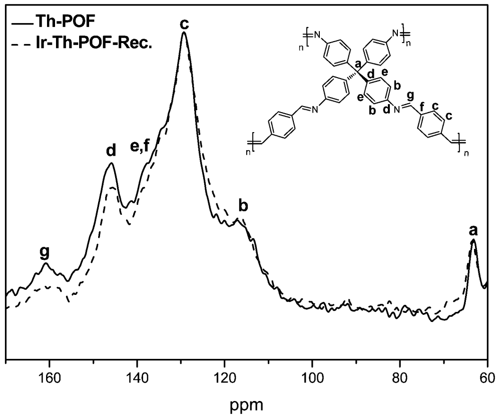

Fig. 9 Solid-state ^{13}C-NMR of **Th-POF** and recycled **Ir-Th-POF**.

The solid-state ^{13}C-NMR of the **Th-POF** was compared with that of the **Ir-Th-POF** (Fig. 9). The **Th-POF** spectrum showed a peak at 63 ppm (a) due to the quaternary spiranic carbon, a group of signals between 117 and 145 ppm (b–f) attributed to the aromatic carbons and the peak due to the C═N at 161 ppm (g). All peaks prevailed in the **Ir-Th-POF** spectrum which showed only a slight shift and peak intensity associated with the imine bond. These results confirmed that the chemical structure prevailed after incorporation of the metal and recycling.

3. Experimental part

3.1 Measurements

Fourier Transform Infrared Spectra (FTIR) of polymers were recorded on a Perkin-Elmer RX-1 instrument. Microanalyses were done with a Carlo Erba EA1108 elemental analyzer (C, H, N). Metal contents were analyzed by Inductively Coupled Plasma Optical Emission Spectroscopy (ICP-OES) on a Perkin Elmer OPTIMA 2100 DV.

Thermogravimetric analysis (TGA) data were obtained on a TGA Q-500 analyzer under air atmosphere, using approximately 5 mg of sample under a flow of 60 mL min^{-1}. The samples were heated from 50 to 850 °C at 10 °C min^{-1}. Specific surface area measurement and porosity analysis were performed using N_2 adsorption isotherms (Micromeritic, ASAP 2020 MICROPORE DRY Analyzer) using the BET technique for surface area calculation and the BJH method for average pore size and pore volume calculations. Wide angle X-ray scattering diagrams were performed on polymers using a Bruker D8 Advance system provided with a Vantec 1 detector. CuKα radiation of wavelength 1.54 Å was used, operating at 40 kV and 40 mA. The angular range was 5–50°.

The solid-state ^{13}C-NMR spectrum of **POFs** was recorded at a MAS rate of 10 kHz in a Bruker AV-400-WB.

Particle morphology and size were studied under a scanning electron microscope (FE-SEM) (SU8000, Hitachi) operating at 0.5 kV. For the SEM measurements, dust particles were deposited on a double sided adhesive. Diffuse reflectance spectra were recorded on a Shimadzu UV-2401PC apparatus.

3.2 Monomers and reagents

The synthesis of 1,3,5-tri(4-aminophenyl)benzene (C_{3v}) was carried out according to the method reported.[29] Tetra-(4-aminophenyl)methane (T_h) was also synthesized following the reported procedure.[30] Terephthalaldehyde was purchased from Aldrich and used as received. Solvents and other reagents were used without further purification.

3.3 Synthesis of POFs

3.3.1 General procedure.

In a round bottomed three-neck flask with mechanical stirring, a water-cooled reflux condenser, a silicone bath and under a nitrogen flow, tetra-(4-aminophenyl)methane (0.50 g, 1.31 mmol, 1 eq.) and anhydrous DMSO (7.4 mL) were added. The reaction mixture was heated at 50 °C, and after 10 minutes stirring at this temperature a solution of 1,4-benzenedicarbaldehyde (0.35 g, 2.62 mmol, 2 eq.) and anhydrous DMSO (3.5 mL, the final concentration of the reaction is 0.48 M with respect to the amino groups) was added dropwise and then the temperature of the bath was increased slowly to 180 °C. After 10 min, a yellow solid precipitated and the reaction was stirred at 180 °C for 48 hours under nitrogen atmosphere to complete condensation. After the reaction was stopped and cooled down to room temperature, the precipitate formed was filtered on a Büchner and it was washed with anhydrous *N*,*N*-dimethylformamide (3 × 50 mL), anhydrous tetrahydrofurane (3 × 50 mL) and anhydrous dichloromethane (3 × 50 mL). **POFs** (730 mg, 93%) were obtained as a yellow solid, which was dried at 120 °C per 1 mm Hg overnight.

3.4 Preparation of catalyst

3.4.1 M-POFs.

A mixture of 5.00 mg of the corresponding metallic salt ($CuCl_2$, CuCl or $[IrCl(COD)_2]$) in THF (15 mL) and **POF** material (50 mg) was stirred at room temperature for 24 h. The solid was then filtered through a G4 sintered glass crucible and washed with EtOH (4 × 5 mL) and ether (4 × 5 mL) to remove any trace amount of unreacted salts. It was then dried in an oven at 80 °C overnight to provide an easy flowing light brown powder. The **POF**-supported metal catalyst showed the following metal contents determined by ICP: **Cu-C3v-POF**, Cu(II) content = 0.41 wt%; **Cu-Th-POF**, Cu(II) content = 2.09 wt%; **Cu-Th-POF**, Cu(I) content = 2.73 wt%; **Ir-C3v-POF**, Ir content = 0.39 wt%; and **Ir-Th-POF**, Ir content = 2.70 wt%.

3.5 Catalytic conditions

3.5.1 General procedure for the cyclopropanation reactions.

The Cu **POF**-catalyst (20 mg of solid catalyst) and the olefin

(0.086 mmol) were suspended in 1 mL of dichloromethane, and 0.129 mmol of the diazo compound [ethyl diazoacetate (EDA) or ethyl 2-phenyldiazoacetate (PhEDA)] in 1 mL of dichloromethane was added either in one portion before starting the reaction or slowly in a dropwise manner with a syringe pump over 2 h. Gas evolution was observed along with a smooth change in color. The resulting mixture was stirred at ambient temperature for 24 h. The reaction was monitored by gas chromatography on HP5890 II GC-MS and Konik HRGC 4000B GC-MS chromatographs with a cross-linked (95%)-dimethyl-(5%)-diphenylpolysiloxane (Teknokroma TRB-5MS) column of 30 meters of length; helium as a carrier gas. 20 psi; injector temperature: 230 °C; detector temperature: 250 °C; oven program for styrene: 70 °C (3 min), 15 °C min^{-1} to 200 °C (5 min); retention times: ethyl diazoacetate 3.20 min, styrene 3.82 min, *n*-decane 5.47 min (internal reference), diethyl maleate 7.84 min, diethyl fumarate 8.02 min, *cis*-cyclopropanes 10.91 min, *trans*-cyclopropanes 11.41 min.

3.5.2 General procedure for the hydrogenation reactions. Catalytic reactions were performed in a reactor (Autoclave Engineers, 100 mL capacity, 1500 RPM). Conversions and selectivities were measured by NMR and gas chromatographic techniques. All hydrogenated products were initially identified by using authentic commercial samples of the expected products. A mixture of the appropriate alkene (2.81 mmol) was introduced into the reactor together with a catalytic amount of Ir-loaded **POF**-catalyst (0.1 mol%) and ethanol, 40 mL). Afterwards, the reactor was sealed and air was purged by flushing three times with 2 bar of hydrogen. Then, the reaction mixture was stirred, heated at 40 °C, and the reactor was pressurized with H_2 at the required pressure. The progress of the reaction was monitored by GC. When the hydrogenation reaction was finished, the reactor was depressurized. Finally, the catalysts were filtered and the organic solution was concentrated under vacuum and analyzed by GC-MS.

3.6 Recycling experiments

At the end of the process the reaction mixture was centrifuged, and the solid residue washed to completely remove any remaining products and/or reactants. The solid was used again without significant changes in the catalytic activity.

4. Conclusions

We have described the use of polymer organic frameworks (**Th-POFs**) as supports to get heterogenized catalysts containing transition metals (**M-Th-POF**; M = Cu(I) or Ir(I)). **M-Th-POFs** turn out to be effective catalysts for reactions such as cyclopropanation or hydrogenation. Recycling experiments with **M-Th-POF** demonstrate that they are truly heterogeneous and reusable catalysts.

Acknowledgements

The financial support provided by the Spanish Ministerio de Ciencia e Innovación (MICINN) (Projects: Consolider CDS2009-050-Multicat, MAT2011-29020-C02-02 and MAT2010-20668) is gratefully acknowledged. We thank Cristina Guerrero for the BET measurements.

Notes and references

1 A. Vinu, T. Mori and K. Ariga, *Sci. Technol. Adv. Mater.*, 2006, **7**, 753–771.
2 S. A. Jenekhe and X. L. Chen, *Science*, 1999, **283**, 372–375.
3 A. S. Zalusky, R. Olayo-Valles, J. H. Wolf and M. A. Hillmyer, *J. Am. Chem. Soc.*, 2002, **124**, 12761–12773.
4 Y. Zhang, L. Zhao, P. K. Patra and J. Y. Ying, *Adv. Synth. Catal.*, 2008, **350**, 662–666.
5 S. A. Johnson, P. J. Ollivier and T. E. Mallouk, *Science*, 1999, **283**, 963–965.
6 Y. Meng, D. Gu, F. Zhang, Y. Shi, H. Yang, Z. Li, C. Yu, B. Tu and D. Zhao, *Angew. Chem., Int. Ed.*, 2005, **44**, 7053–7059.
7 F. Schüth, *Chem. Mater.*, 2001, **13**, 3184–3195.
8 F. X. Simon, N. S. Khelfallah, M. Schmutz, N. Díaz and P. J. Mésini, *J. Am. Chem. Soc.*, 2007, **129**, 3788–3789.
9 Z. Yang, J. Wang, K. Huang, J. Ma, Z. Yang and Y. Lu, *Macromol. Rapid Commun.*, 2008, **29**, 442–446.
10 P. J. Flory, *J. Am. Chem. Soc.*, 1952, **74**, 2718–2723.
11 S. Russo, A. Boulares and A. Mariani, *Macromol. Symp.*, 1998, **128**, 13–20.
12 M. Jikei, S. H. Chon, M. Kakimoto, S. Kawauchi, T. Imase and J. Watanebe, *Macromolecules*, 1999, **32**, 2061–2064.
13 J. Gen, M. Yan, D. Lu, M. Zhang and Z. Liu, *Biochem. Eng. J.*, 2007, **36**, 93–99.
14 Q. Lin and T. E. Long, *Macromolecules*, 2003, **36**, 9809–9816.
15 S. Unal, Q. Lin, T. H. Mourey and T. E. Long, *Macromolecules*, 2005, **38**, 3246–3254.
16 W. Lu, D. Yuan, D. Zhao, C. I. Schilling, O. Plietzsch, T. Muller, S. Bräse, J. Guenther, J. Blümel, R. Krishna, Z. Li and H. C. Zhou, *Chem. Mater.*, 2010, **22**, 5964–5972.
17 M. G. Rabbani and H. M. El-Kaderi, *Chem. Mater.*, 2011, **23**, 1650–1653.
18 P. Kuhn, M. Antonietti and A. Thomas, *Angew. Chem., Int. Ed.*, 2008, **47**, 3450–3453.
19 J. X. Jiang, F. Su, A. Trewin, C. D. Wood, H. Niu, J. T. A. Jones, Y. Z. Khimyak and A. I. Cooper, *J. Am. Chem. Soc.*, 2008, **130**, 7710–7720.
20 F. J. Uribe-Romo, J. R. Hunt, H. Furukawa, C. Klöck, M. O'Keeffe and O. M. Yaghi, *J. Am. Chem. Soc.*, 2009, **131**, 4570–4571.
21 P. Pandey, A. P. Katsoulidis, I. Eryazici, Y. Wu, M. G. Kanatzidis and S. T. Nguyen, *Chem. Mater.*, 2010, **22**, 4974–4979.
22 S. Y. Ding, J. Gao, Q. Wang, Y. Zhang, W. G. Song, C. Y. Su and W. Wang, *J. Am. Chem. Soc.*, 2011, **133**, 19816–19822.
23 P. N. Basa, A. Bhowmick, M. M. Schulz and A. G. Sykes, *J. Org. Chem.*, 2011, **76**, 7866–7871.
24 H. S. Jung, K. C. Ko, J. H. Lee, S. H. Kim, S. Bhuniya, J. Y. Lee, Y. Kim, S. J. Kim and J. S. Kim, *Inorg. Chem.*, 2010, **49**, 8552–8557.
25 K. H. Lee, C. S. Choi and K. S. Jeon, *J. Photosci.*, 2002, **93**, 71–74.
26 C. J. Yeng and S. A. Jenekhe, *Macromolecules*, 1995, **28**, 1180–1196.
27 A. M. Gad, A. El-Dissouky, E. M. Mansour and A. El-Maghraby, *Polym. Degrad. Stab.*, 2001, **71**, 267–272.
28 M. J. Alcón, A. Corma, M. Iglesias and F. Sánchez, *J. Organomet. Chem.*, 2002, **655**, 134–145.
29 Z. Wang, B. Zhang, H. Yu, G. Li and Y. Bao, *Soft Matter*, 2011, **7**, 5723–5730.
30 O. K. Farha, A. Spokoyny, B. G. Hauser, Y. S. Bae, S. E. Brown, R. Q. Snurr, C. A. Mirkin and J. T. Hupp, *Chem. Mater.*, 2009, **21**, 3033–3035.